Expression and estrogen regulation of G protein-coupled estrogen receptor in human glioblastoma cells

KARLA MARIANA PEÑA-GUTIÉRREZ[1], KARINA HERNÁNDEZ-ORTEGA[2],
CLAUDIA BELLO-ALVAREZ[1] and IGNACIO CAMACHO-ARROYO[1]

[1]Unidad de Investigación en Reproducción Humana, Instituto Nacional de Perinatología-Facultad de Química, and
[2]Departamento de Biología, Facultad de Química, Universidad Nacional Autónoma de México, 11000 Mexico City, Mexico

Abstract. Glioblastoma (GB) is the most frequent primary brain tumor with a very poor prognosis. Sex hormones are crucial players in the development of GBs. 17 β-estradiol (E2) signaling is involved through its corresponding intracellular receptors [estrogen receptor α (ERα) and β (ERβ)] in GB cell proliferation and progression. E2 activates G-protein coupled estrogen receptor (GPER), leading to rapidly occurring effects, independently of gene transcription. GPER activation is involved in tumor progression in various cancer types. Currently, available data concerning the occurrence and role of GPER in GB are very limited. In the present study, it was observed that GPER was expressed in human brain tumor cell lines [U251 (astrocytoma-derived cell line), U87, LN229 and T98 (glioblastoma-derived cell line)]. Immunofluorescence assays revealed that GPER localizes in the plasma membrane, cytoplasm and nucleus. An *in silico* analysis identified two potential E2 response elements in the promoter region of the GPER gene. E2 increased GPER expression in the U251, U87 and LN229 cell lines. Molecular modeling data derived from *in silico* analysis predicted the three-dimensional conformation of GPER, and docking analysis identified potential binding sites of E2 and its specific agonist, G1. Taken together, these results indicate that GPER may be differentially expressed in human GB cell lines with E2 possibly upregulating GPER expression. The present study raises further questions about the implications of GPER-mediated E2 signaling in the biology of GBs.

Correspondence to: Dr Ignacio Camacho-Arroyo, Unidad de Investigación en Reproducción Humana, Instituto Nacional de Perinatología-Facultad de Química, Universidad Nacional Autónoma de México, C. Montes Urales 800, Lomas-Virreyes, Lomas de Chapultepec IV Secc, Miguel Hidalgo, 11000 Mexico City, Mexico
E-mail: camachoarroyo@gmail.com

Introduction

Glioblastoma (GB) is widely known as the most frequent and lethal primary brain tumor affecting adults. The overall survival rate of patients with GB does not exceed 15 months. The prevalence of GB is significantly higher among males than females at a ratio of 1.6/1 (1); this sex-dependent difference may indicate a role of sex hormones in the incidence and progression of GB, in particular as regards 17 β-estradiol (E2), which is the most potent estrogen, and which has been most frequently studied in this context (2). E2 promotes cell proliferation, migration and invasion in human GB (2-4). However, E2 has been reported to exert diverse effects on GB, depending on the concentration (3,5) and the predominant signaling of the intracellular receptor subtype [estrogen receptor α (ERα) and β (ERβ)]. In general, the prevalence of ERα signaling has been found to be associated with GB progression, while E2 signaling by ERβ has been shown to be associated with anti-neoplastic effects (3,6,7), González-Arenas *et al* (3) demonstrated that ERα and not ERβ activation increased the proliferation of human astrocytoma-derived cells. More recently, Hernández-Vega *et al* (6) described that ERα activity, in contrast to ERβ activity, promoted epithelial-mesenchymal transition (EMT) in human GB cells. Signaling pathways of E2 can also proceed through G-protein coupled estrogen receptor (GPER), a seven-transmembrane domain protein that leads to rapid effects, independently of gene transcription. In 1996, the orphan GPCR30 was discovered (GPR30) (8). In a subsequent study, estrogen binding to GPR30 was reported; therefore, it was renamed as GPER (9). Following ligand binding, GPER signaling proceeds through various non-genomic pathways (10). The protective effects of GPER against brain injury have been reported. In primary cortical neuron cultures, GPER activation has been shown to exert neuroprotective effects against excitotoxic stimuli (11). Notably, there is evidence of cross-regulation between intracellular and membrane E2 receptors (ERα, ERβ and GPER) (12). In zebrafish, the process of vitellogenesis is regulated by ERα and its interaction with ERβ and GPER (13). In human renal tubule epithelial cells, E2 increases proliferation through the co-operative actions

between ERα and GPER (14). This phenomenon extends to the context of cancer, where the interplay between GPER and ERα in promoting tumor progression has also been observed (15).

The role of GPER in cancer has been studied in various malignancies. In ovarian cancer, the high expression of GPER has been found to be associated with a poor survival rate (16). In triple-negative breast cancer, GPER/ERK signaling has been shown to promote tumor progression (11,17). In human lung cancer cells, the GPER/EGFR/ERK1/2 pathway induces the upregulation of matrix metalloproteinases, proteins essential in invasion and metastasis (18). Avino *et al* (19) reported that insulin-like growth factor-I (IGF-I)/IGF-I receptor (IGF-IR) and GPER functioned together to promote migration in mesothelioma and lung cancer. However, in the context of GB development, evidence of the regulation and functions of GPER is limited. Recently, Hirtz *et al* (20) reported GPER protein expression in the human GB-derived cell lines, U251 and LN229. In the present study, the expression of GPER in U251, U87, LN229 and T98 human GB-derived cell lines was evaluated at the mRNA and protein levels and GPER subcellular localization was determined. It was also examined whether E2 could regulate GPER expression by identifying two estrogen response elements (EREs) in the GPER promoter through an *in silico* analysis, and the regulation of GPER expression by E2 in GB-derived cell lines was determined. Furthermore, potential GPER structure models for molecular docking of the predicting binding sites for E2 and the synthetic GPER ligand, G1, were obtained by an *in silico* analysis.

Materials and methods

Cell culture and treatments. The U251 astrocytoma cell line, the LN229 (CRL-2611) and T98G (CRL-1690) glioblastoma cell lines, and the U87 cell line (HTB-14, glioblastoma of unknown origin) were purchased from the American Type Culture Collection (ATCC). The U251 and U87 cell lines were previously authenticated by the authors using STR profiling. All cells were cultured up to 25-30 passages, evaluating morphological characteristics maintenance and monitoring routinely for mycoplasma contamination (data not shown) by microscopic examination. In addition, all cell lines were cultured in Dulbecco's modified Eagle's medium (DMEM) with phenol red (Biowest) supplemented with 10% fetal bovine serum (FBS), 1 mM sodium pyruvate (Biowest), 0.1 mM non-essential amino acids (Invitrogen; Thermo Fisher Scientific, Inc.), and 1 mM antibiotic (streptomycin 10 g/l; penicillin G 6.028 g/l; and amphotericin B 0.025 g/l, Biowest, cat. no. L0010). Cells were incubated under standardized conditions of 37˚C, 95% air, 5% CO_2 and 95% humidity. Cells were cultured until a confluence of 70-80%. Afterwards, the medium was changed to phenol red-free DMEM (Invitrogen; Thermo Fisher Scientific, Inc.), supplemented with 10% hormone-free FBS, 0.1 mM non-essential amino acids (Invitrogen; Thermo Fisher Scientific, Inc.), and 1 mM antibiotic, used for a 24-h cell incubation. Subsequently, E2 (E4389, MilliporeSigma) or vehicle (cyclodextrin; MilliporeSigma) were added at 1, 10, 100 nM and 1 μM for 24 h, and total RNA or total protein extraction was performed.

RNA extraction and reverse transcription-quantitative polymerase chain reaction (RT-qPCR). RNA extraction from U251, U87, LN229 and T98 cell lines was performed using TRIzol® reagent (Invitrogen; Thermo Fisher Scientific, Inc.) following the manufacturer's instructions. Total RNA of healthy human astrocytes (HA) obtained from ScienCell Research Laboratories, Inc. was used to compare GPER mRNA levels. A total of one μg of total RNA was used to synthesize the first-strand cDNA in a reaction with M-MLV reverse transcriptase (Thermo Fisher Scientific, Inc. cat. no. 28025013) following the manufacturer's protocol. GPER relative expression to the 18S ribosomal RNA (rRNA) was determined using RT-qPCR with standardized primers for GPER (21) as follows: Forward, 5'-TCACGGGCCACATTGTCAACCTC-3' and reverse, 5'-GCTGAACCTCACATCCGACTGCTC-3'; 18S forward, 5'-AGTGAAACTGCAATGGCTC-3' and reverse, 5'-CTG ACCGGGGTTGGTTTTGAT-3'. For RT-qPCR, the FastStart D.N.A. Master SYBR-Green I kit (Roche Diagnostics GmbH) was used to perform amplification in the Light Cycler 2.0 (Roche Diagnostics). The following thermocycling conditions were applied for RT-qPCR: 95˚C for 10 min, followed by 35 amplification cycles of 95˚C for 10 min, 62˚C for 10 sec, and 72˚C for 10 sec. The relative expression of the GPER gene was calculated, considering the 18S rRNA gene as an endogenous expression control reference. Relative expression was quantified using the comparative method of $2^{-\Delta\Delta Cq}$ (22,23).

Protein extraction and western blot analysis. The content of GPER protein was determined using western blot analysis in U251, U87, LN229 and T98 cell lines. Following the treatments (E2 1, 10, 100 nM and 1 μM), cells were homogenized in RIPA buffer with a cocktail of protease inhibitors (MilliporeSigma). Proteins were obtained by centrifugation at 16,500 x g at 4˚C for 5 min and quantified using the NanoDrop 2000 spectrophotometer (Thermo Fisher Scientific, Inc.). Also, a total HA protein extract from ScienCell Research Laboratories, Inc. (cat. no. 1806) was used. A total protein quantity of 30 μg per lane was loaded on a 12% polyacrylamide gel under denaturing conditions for protein separation. Proteins were transferred to a nitrocellulose membrane (Bio-Rad, cat. no. 1620115) under semi-dry conditions for 45 min at 25 V. Blocking was completed with 5% bovine serum albumin (BSA; Gold Biotechnology) at 37˚C for 2 h. Membranes were incubated with the primary antibody against GPER (1:400; cat. no. ab39742; Abcam) at 4˚C for 48 h. As a loading control, the α-tubulin protein content (1:1,000, at 4˚C for 24; sc-398103, Santa Cruz Biotechnology, Inc.) was determined. Subsequently, all membranes were incubated with the anti-rabbit IgG (1:10,000; cat. no. 1858415; Thermo Fisher Scientific, Inc.) or anti-mouse IgGMκ (1:10,000; cat. no. sc-516102; Santa Cruz Biotechnology, Inc.) secondary antibodies at room temperature for 45 min, with shaking. The secondary antibodies were removed, and the membranes were washed (TBS with 0.1% Tween). Finally the signal was detected with Super Signal West Femto Maximum Sensitivity Substrate (Thermo Fisher Scientific, Inc.) and quantified. Densitometric analysis of the western blot bands was performed with Image J 1.45S software (National Institutes of Health, USA). The content of GPER was normalized concerning the α-tubulin.

Immunofluorescence. A total number of 15x10³ U87 cells per well were seeded on coverslips in DMEM medium (Invitrogen, Thermo Fisher Scientific, Inc.) supplemented with 10% FBS,

1 mM pyruvate, 2 mM glutamine, and 0.1 mM non-essential amino acids (Gibco; Thermo Fisher Scientific, Inc.) and with 1% penicillin/streptomycin at 37˚C with 5% CO_2. Following a 24-h incubation, the medium was changed with DMEM medium without phenol red, FBS and antibiotics. Afterwards, following a further 24-h incubation in this medium, the cells were incubated in a blocking solution (PBS with 1% BSA, MilliporeSigma) at 37˚C for 20 min. Some experiments were performed in permeabilized conditions by adding 0.2% Triton (MilliporeSigma). Subsequently, the cells were incubated with a polyclonal rabbit anti-GPER (1:350; cat. no. ab39742; Abcam) in a PBS solution with 1% glycine (MilliporeSigma) and 1% BSA (MilliporeSigma) for 24 h. Upon the removal of the primary antibody, the cells were washed with PBS and incubated with 568-conjugated goat anti-rabbit IgG (1:400; Thermo Fisher Scientific, Inc.) at room temperature for 60 min. The cells were then washed and incubated with Hoechst (1 mg/ml; 33342, Thermo Scientific, USA) at room temperature for 7 min. Finally, the cells were washed and mounted in Aqua-Poly/Mount medium (cat. no. 18606; Polysciences, Inc.). Slides were observed under a Nikon A1R confocal microscope. Four different arbitrary fields were captured for all experimental conditions, and a Z-reconstruction with an orthogonal and 3D projection was obtained at a total magnification of x600. Fluorescence intensity analysis of the images was performed with ImageJ® 1.45S software (National Institutes of Health). At least three cells per field were analyzed. To calculate the fluorescence intensity, the formula of corrected total cell fluorescence (CTCF) was used: CTCF=integrated density-(area of selected cell x average background fluorescence) (24). The percentage of the GPER positive area included the regions of interest (ROIs) in each cell analyzed. Negative control with the use of secondary antibody only was also performed.

Prediction of EREs. The GPER gene sequence was obtained from the National Center for Biotechnology Information (NCBI) database, entry NC_000007.14: 1085755-1094865, by using the entire promoter region for analysis. Probability matrices for EREs were obtained from the JASPAR (25), HOMER (26) and HOCOMOCO (27) platforms. Data were analyzed using the TFBSTools package (28) for R v4.0.2 on windows. Sites with a score ≥0.9 and predicted by at least two matrices were considered as possible EREs. The generated bed files were visualized using Integrative Genomics Viewer v2.8.7 software (Broad Institute) (29).

Molecular modeling of GPER and docking. The amino acid sequence of GPER was obtained from the UniProtKB database (Q99527, GPER1_HUMAN). A non-redundant alignment was performed using the Protein Data Bank (PDB) database on the Blast-P platform (NCBI), determining three templates in total. Two templates belonged to bovine Rhodopsin crystallographic structures with PDB (entries 1F88 and 1HZX, respectively), with an identity percentage of 23.4%, and one template belonged to a human GPCR PDB (entry 6LFL) with 36.6% identity after alignment. These three structures obtained from PDB were prepared for further use in Chimera (30). For molecular modeling by homology, Modeller software (31,32) was used with a base script. A total of 50 models were obtained for each one of the three

obtained templates. Model validation was carried out using the Hammer program (Rd. Hmmr) (33) in Linux and the Prosa-web server (34), selecting the models with the best score. The selected models were visualized with Visual Molecular Dynamics (VMD) (35), and representations of each model were obtained, indicating the regions of interest in each structure. These models were prepared in the Auto-Dock Tools (36) for Linux distribution ubuntu 20.04 to obtain the pdbqt files with rigid residues for subsequent use in docking analysis. E2 (ID:5757) and 1-((3aS,4R,9bR)-4-(6-bromo-1,3-benzo-dioxol-5-yl)-3a,4,5,9b-tetrahydro-3H-cyclopenta (c) quinolin-8-yl) ethanone, G1 (ID: 5322399) ligands were obtained in sdf format from the PubChem (NCBI). The pdb files for these ligands were obtained using the Open Babel v.2.3.1 (37). Subsequently, the structures of the ligands were prepared using Chimera and Autodock Tools, acquiring the pdbqt files for each ligand. At this point, blind docking was performed by defining the Grid box for the entire extracellular region using AutoDock 4 (38). The parameter search was performed using a Lamarckian genetic algorithm (LGA), and mean completeness (250,000) and 100 run poses were determined. Finally, the data resulting from the clusters for the conformations of each ligand in each model were evaluated, taking as the best binding energy those values that presented the highest number of conformations.

Statistical analysis. Data were analyzed using one-way ANOVA followed by Tukey's multiple comparisons test. GraphPad Prism 5.0 software (GraphPad Software, Inc.) was used to perform the statistical analyses. Results are expressed as mean ± SEM (n=5). $P < 0.05$ was considered to indicate a statistically significant difference.

Results

Characterization of mRNA levels and protein content of GPER in human astrocytoma and GB tumor cell lines. To characterize the expression of GPER in four GB-derived cell lines (U251, U87, LN229 and T98), mRNA levels and protein content were measured using RT-qPCR and western blot analysis, respectively. GPER mRNA and protein expression was detected in all cell lines under common culture conditions (Fig. 1A and B). The GPER mRNA levels in HA were significantly higher than those in GB-derived cell lines (Fig. 1A). At the protein level, two bands corresponding to the reported molecular weights of GPER (70 and 55 kDa) were detected (Fig. 1B). The presence of different GPER isoforms has been shown to be related to receptor maturation through N-glycosylation (39-41). Densitometric analysis indicated that the U87 cells showed the highest protein content of GPER in 55 kDa band) (Fig. 1B and C).

Subcellular localization of GPER in a human GB-derived cell line. To further elucidate the subcellular localization of GPER in GB cells, the U87 cells were evaluated (since these cells demonstrated the highest GPER content according to Fig. 1B-D) by immunofluorescence and confocal microscopy. In non-permeabilized cells, GPER was localized in the plasma membrane and at the edge of the cell (Fig. 2A). By contrast, GPER was also observed in the nucleus of permeabilized cells,
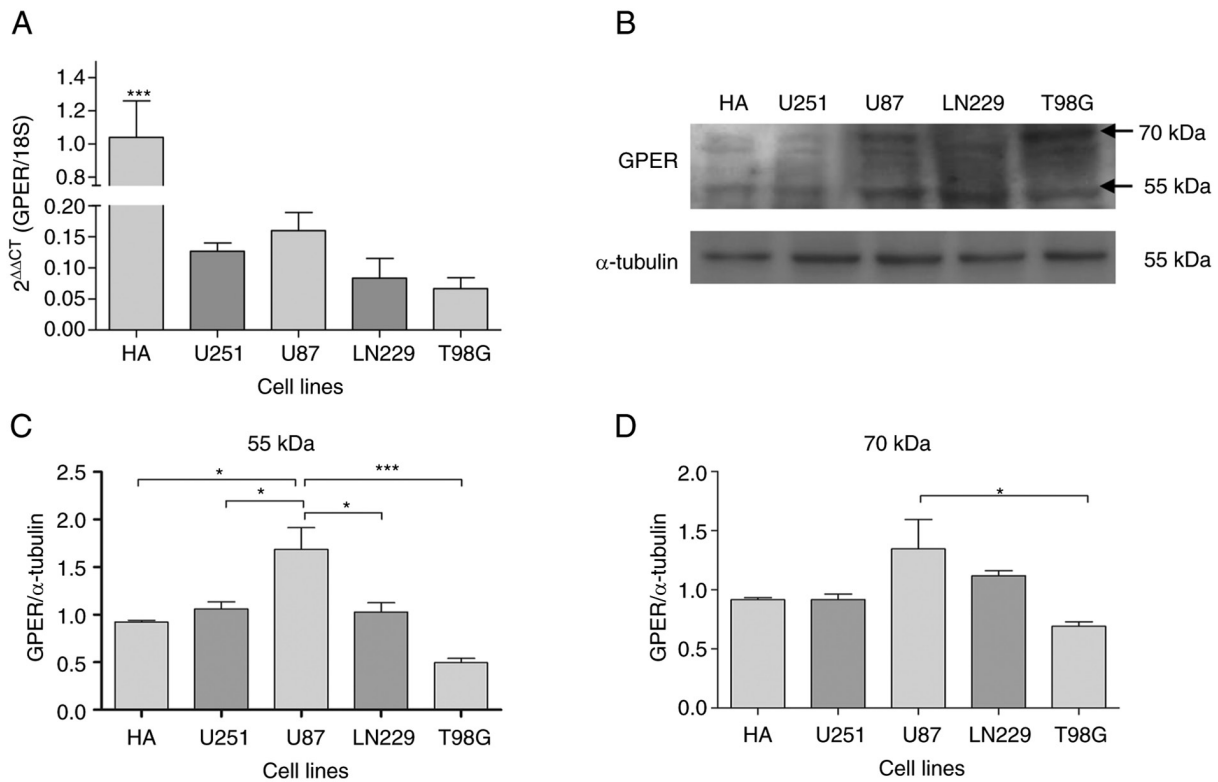
Figure 1. Characterization of GPER expression in human GB-derived cell lines. (A) GPER mRNA levels (normalized to 18S rRNA levels by applying $2^{-\Delta\Delta Cq}$ method) in HA, human GB-derived cell lines (U87, LN229 and T98), and a human astrocytoma cell line (U251). Each bar represents the mean ± SEM (***P<0.001 vs. the tumor cell lines). (B) Representative western blots for the GPER (70 and 55 kDa) content. (C and D) Densitometric analysis of the GPER western blots for the 70 and 55 kDa bands, respectively. Data were normalized in relation to the HA cell line values. Results are expressed as the mean ± SEM, n=3 (*P<0.05). GPER, G-protein coupled estrogen receptor; HA, healthy human astrocytes.

as it colocalized with Hoechst dye, as shown in (Fig. 2C). The CTCF indicated a higher fluorescence intensity in the nucleus than in the cytoplasm of permeabilized cells (Fig. 2D). On the other hand, the analysis of the GPER-positive area demonstrated a decreased distribution percentage in the cell nucleus compared with the cytoplasm (Fig. 2E).

GPER promoter region contains two ERE sequences. In order to investigate the potential effect of E2 on GPER expression in human GB cell lines, an *in silico* analysis with TFBSTools was performed to identify EREs (28). The analysis indicated two potential EREs with a score equal to or greater than 0.9 and whose sequences were predicted in at least two of the three used matrices (JASPAR, HOMER and HOCOMOCO). The sequences and position of these putative binding sites are presented in Fig. 3A and B.

E2 increases GPER expression in human GB-derived cell lines. In order to evaluate whether E2 regulates GPER expression in brain tumor cells, the U251, U87, LN229 and T98 cell lines were treated with various E2 concentrations (1, 10 and 100 nM, and 1 μM). It is worth mentioning that in all experimental conditions, including E2 treatments (under culture conditions with phenol red-free DMEM and hormone-free FBS), the band corresponding to the 70-kDa molecular weight was the most consistently detected (Fig. S1). Therefore, it was used for the analysis of GPER content following E2 treatments. The GPER content (70 kDa)

increased in the U251 and U87 cell lines treated with E2 (10 nM) compared to the vehicle (Fig. 4A and B), while in the LN229 cell line, GPER expression (70 kDa) increased following treatment with 1 μM E2 (Fig. 4C). In the T98G cell line, E2 treatments did not induce any significant change in the GPER content (Fig. 4D). These results suggest that E2 differentially regulates the expression of GPER in human brain tumor cell lines.

Molecular modeling of GPER. At present, there is no crystallographic structural resolution of GPER, to the best of our knowledge. In order to analyze the molecular characteristics of GPER in its three-dimensional conformation *in silico* and suggest *in vivo* receptor behavior, molecular modeling by homology of GPER was performed, using the Modeller program, visualizing the seven-transmembrane domains of GPER protein and the extracellular and intracellular structural regions. The structural conformation of the transmembrane region was conserved in the three templates used for modeling (1F88, 1HZX and 6LFL). However, the structural conformation of the first 50 amino acids was different, depending on the template used. The asparagine residues 25, 32 and 44 in the N-terminal region were defined as glycosylation targets (Fig. 5).

Molecular docking of GPER-ligand interaction. The binding site and affinity of E2 and G1 molecules for GPER have not, to the best of our knowledge, been previously defined. In the present study, a molecular docking and recognition of both
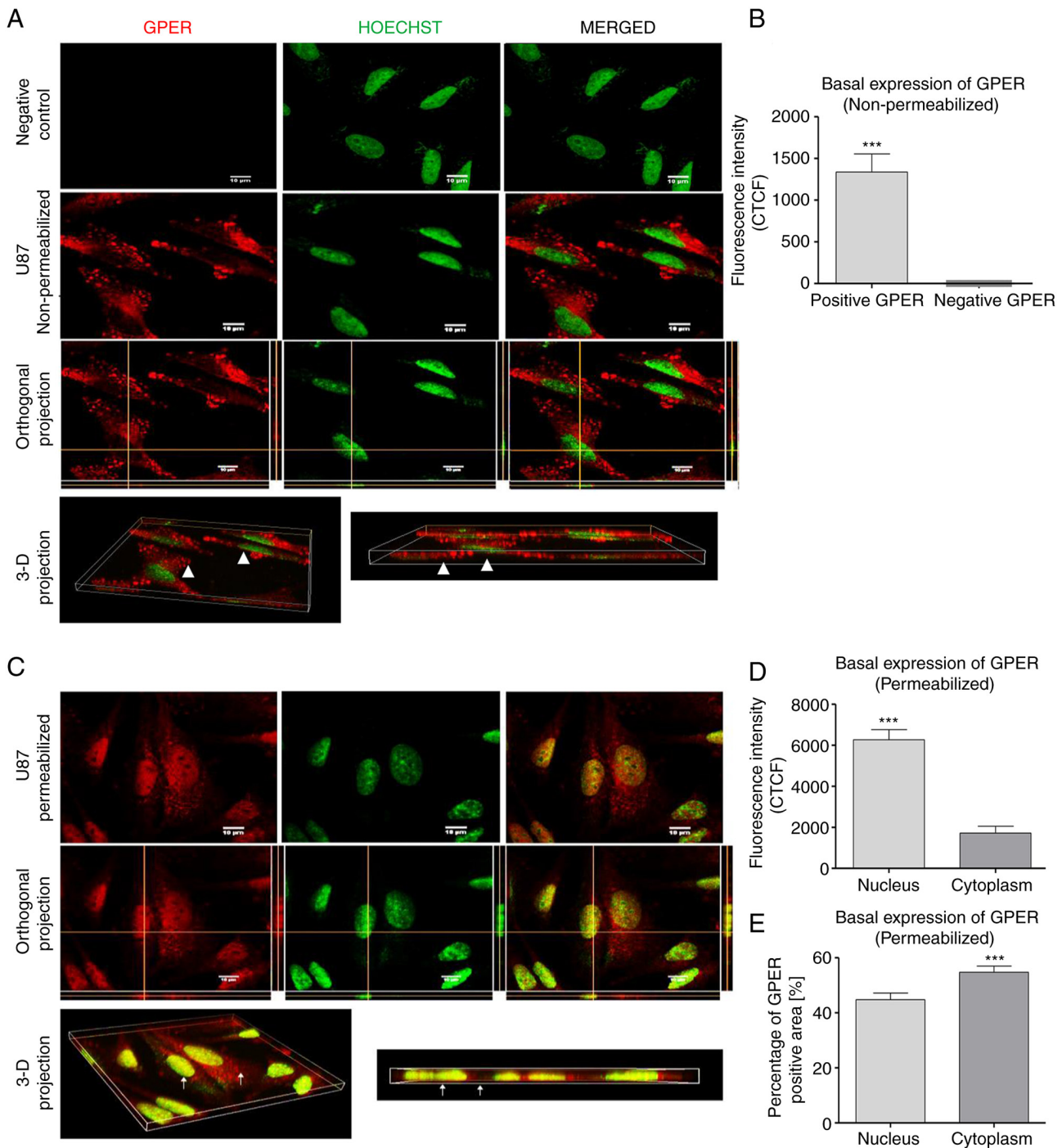
Figure 2. Subcellular localization of GPER in non-permeabilized and permeabilized U87 cells. (A) In non-permeabilized cells, GPER aggregates (red) were mainly observed at the edge of the cell and on the rest of the cell surface. In the merged image, there was no presence of GPER in the nucleus (green); likewise, in the orthogonal projection, in which the intersections of the yellow lines corresponded to the point in the XZ, YZ. plane, which confirmed that in the position of the nucleus there was no presence of GPER (white arrows indicate the nucleus or cytoplasm). (B) Total CTCF analysis of the positive and negative GPER areas in the analyzed images. (C) GPER aggregates (red) were observed in the nucleus and cytoplasm of permeabilized cells (white arrows indicate the nucleus or cytoplasm). (D) CTFC analysis demonstrated a higher fluorescence intensity of GPER was the nucleus than in the cytoplasm. (E) Analysis of the subcellular distribution of the GPER-positive area indicated a lower distribution percentage in the nucleus than in the cytoplasm. Scale bar, 10 μM. Results are expressed as the mean ± SEM, n=3 ([***]P<0.001 vs. negative GPER or cytoplasm). GPER, G-protein coupled estrogen receptor; CTCF, corrected total cell fluorescence.

ligands were conducted, based on the three templates generated for GPER bovine rhodopsin crystallographic structures (PDB entry numbers 1F88 and 1HZX) and one structure of a human GPCR (PDB entry 6LFL). GPER-ligand interaction analysis revealed that in templates 1F88 and 1HZX, E2 and G1 binding occurred in an extracellular domain, while according to the 6LFL template, this binding occurred in the transmembrane region (Fig. 6A). By using the Auto Dock 4 program and Auto Dock Tools, ligand conformations (E2 or G1) with different affinities for each of the receptor models were observed. The highest binding energy for E2 and G1 was observed in the 6LFL template (Fig. 6B). An analysis of the interaction
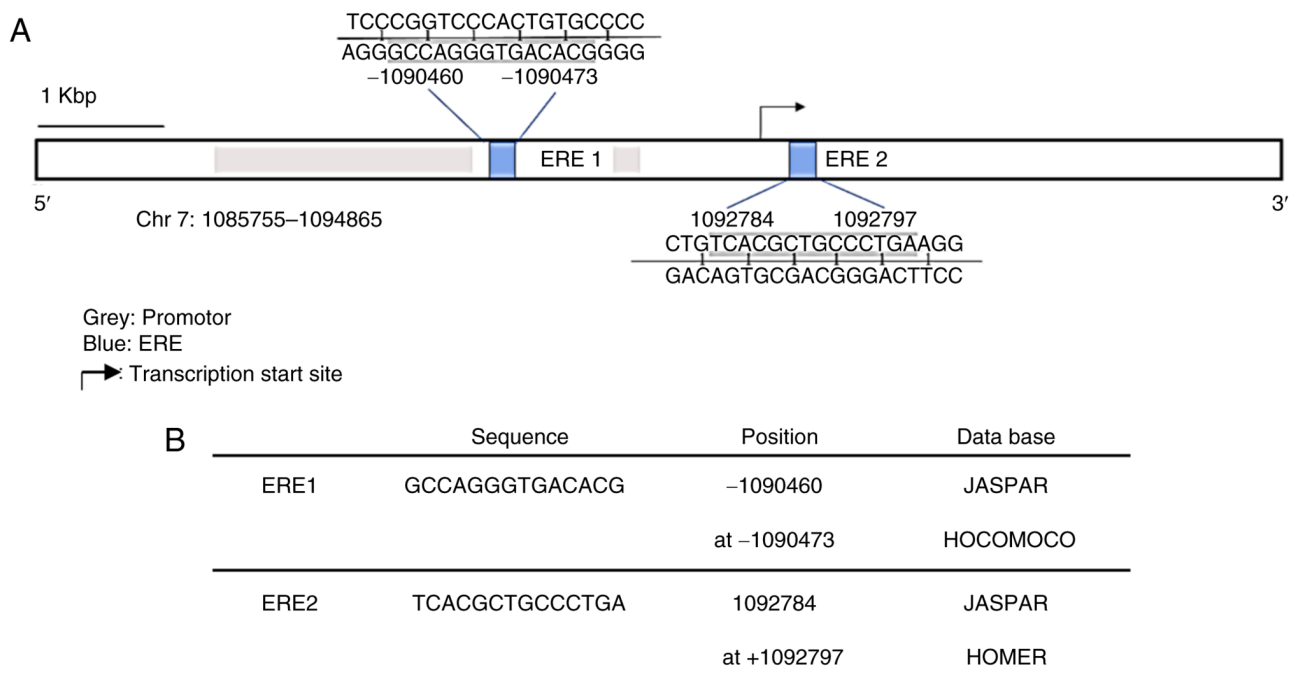
Figure 3. Prediction of EREs in the GPER gene. (A) Schematic representation of the GPER gene. The ERES predicted by *in silico* analysis are marked in blue, and the promoter regions (1086600-1089001 bp and 1090400-1090601 bp) are marked in gray. The black arrow points to the transcription start site. Scale bar, 1 Kbp (kilobase pair). (B) Sequence and position of the two potential EREs predicted by the two databases are indicated. EREs, estrogen response elements; GPER, G-protein coupled estrogen receptor.

sites of each GPER model (1F88, 1HZX, and 6LFL) with both ligands (E2 and G1) was also performed (Fig. 6C and D). In the 1F88 model, E2 and G1 interacted with ALA22, ALA23, SER28, PRO36, GLY39, and THR40 residues. The cluster plot indicated that the most favorable binding energy was -8.1 for E2 and -7.8 for G1. For the 1HZX model, E2 and G1 demonstrated a shared interaction with HIS300, HIS302, and PRO303 residues. Moreover, their favorable binding energies were lower in comparison with a value of -6 for E2 and -6.7 for G1. According to 1F88 and 1HZX models, the binding sites for both ligands are similar. Finally, the 6LFL model revealed that E2 and G1 appear to interact in different regions of GPER. This analysis indicated favorable binding energies, -10.7 for E2, and -10.1 for G1. The highest binding energy of E2 and G1 in the highest number of conformations was obtained with the 6LFL model (Fig. 6D). According to the 6LFL model, E2 and G1 (in the largest number of conformations) presented the highest binding energy of the three models.

Discussion

The present study characterized GPER expression at the mRNA and protein level in three human GB-derived cell lines (U87, T98G and LN229) and one astrocytoma cell line (U251). Moreover, it was explored whether E2 may regulate GPER expression through a genomic mechanism via EREs, and the three-dimensional conformation of GPER and the potential interaction sites with their ligands, E2 and G1, were predicted.

Firstly, GPER expression in the U251, U87, LN229 and T98G human brain tumor cell lines and HA cell line was determined at the mRNA level, the highest expression of GPER was detected in HA, while U87 cells demonstrated the highest expression at the protein level. These results could be related to the cellular heterogeneity of GBs (42-44). However, the functional significance of the increased GPER expression in U87 cells required further evaluation. In ovarian cancer, the higher expression of GPER has been associated with MMP-9 expression, which participates in invasion and migration processes (45). The two bands detected for GPER correspond to the reported molecular weights of GPER (70 and 55 kDa). Gonzalez de Valdivia *et al* (46) described that the GPER reaches a molecular mass of 70-kDa due to glycosylation of the asparagine 44 residue and identified receptor species at a molecular mass of 40 and 110 kDa, as a result of deglycosylation. Other authors have also identified the receptor at 55-kDa molecular weight, suggesting that different GPER species are related to receptor maturation through N-glycosylation (39,40). It would be of interest to evaluate the functional significance of GPER glycosylation in future studies.

The subcellular localization of GPER were also characterized in the U87 cell line. In permeabilized and non-permeabilized preparations, orthogonal projections and 3-D reconstructions indicated that GPER was located in the cytoplasm and the nucleus. In another study the presence of GPER in these compartments has also been reported (47). The results of the present study revealed that in non-permeabilized cells, GPER could only be observed in the plasma membrane, particularly in the prolongations of border cells. Furthermore, according to a previous study on breast cancer cells and in breast cancer-associated fibroblasts, GPER subcellular localization was shown to be related to different tumor properties, with the cytoplasmic expression of GPER associated with a low tumor stage and a better histological differentiation (47-50).
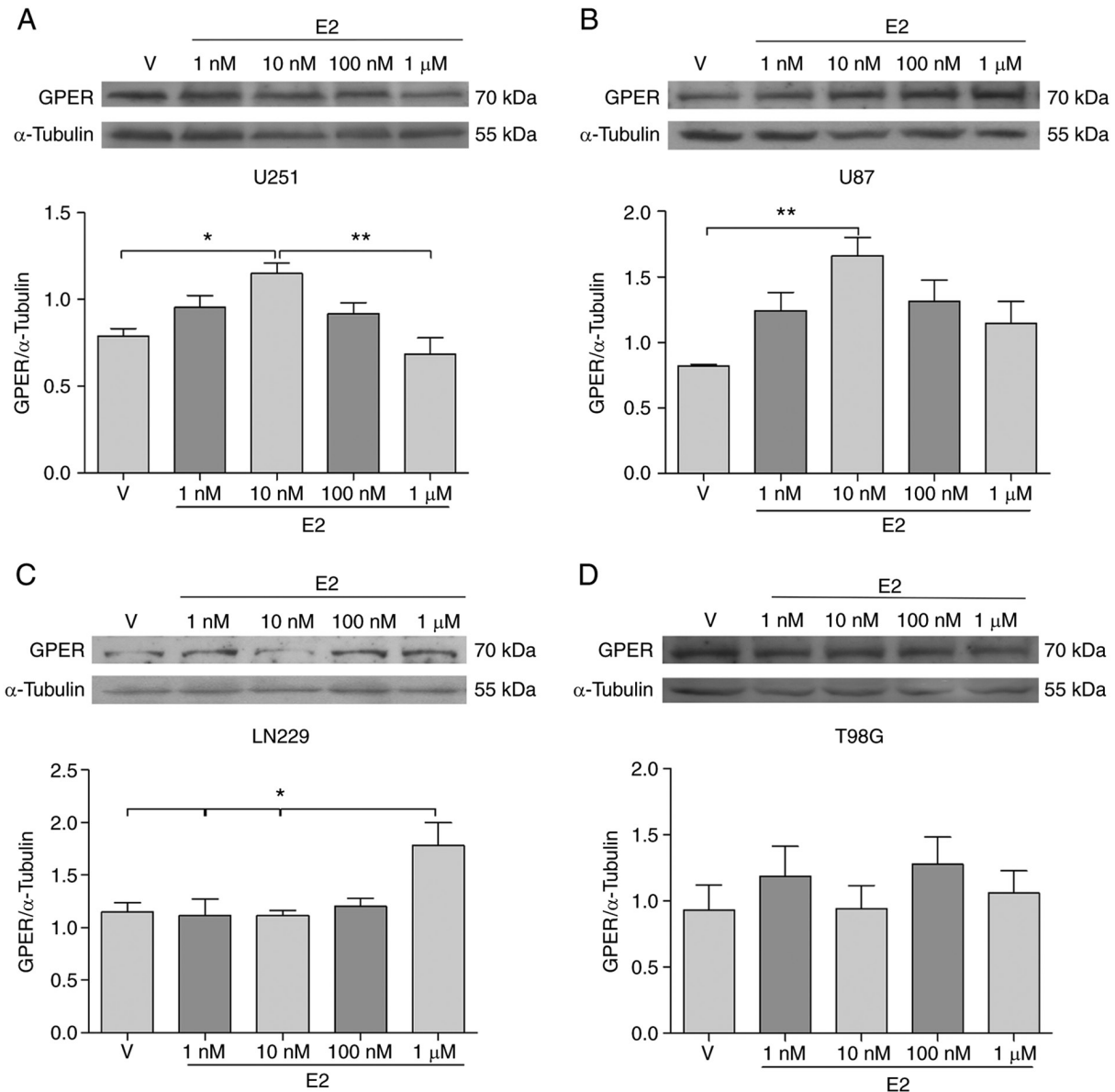
Figure 4. The expression of GPER is modified by E2 treatment in human GB-derived cell lines and an astrocytoma cell line. (A) U251, (B) U87, (C) LN229, and (D) T98G cells were treated with E2 (1, 10 and 100 nM, and 1 μM) or V (cyclodextrin) for 24 h. The upper panels illustrate the representative western blots for GPER and α-tubulin. The lower panels demonstrate the corresponding results of the densitometric analysis. Results are expressed as the mean ± SEM, n=5 (*P<0.05 and **P<0.01). GPER, G-protein coupled estrogen receptor; V, vehicle.

The intracellular trafficking pathway of GPER is highly unusual, as these types of receptors are typically recycled to the plasma membrane or degraded in lysosomes (46,47,51). It has also been described that GPER endocytoses from the plasma membrane through clathrin-coated vesicles, entering early endosomes, and accumulating in a perinuclear compartment; it has also been observed that GPER internalization may occur in the absence of ligand, indicating that the GPER undergoes a constitutive endocytosis (46,47,51-53).

The presence of GPER in the nucleus may also be related to an active transcriptional role of GPER, similar to that first reported by Madeo and Maggiolin (49), who suggested that the localization of GPER and EGFR in the nucleus of breast cancer-associated fibroblasts (CAFs) was necessary for their recruitment to the cyclin D1 promoter sequence. They demonstrated that the functional role of

the nuclear interaction between GPER and EGFR was induced by E2. In another study on breast CAFs, it was reported that GPER translocated to the nucleus through an importin-dependent mechanism, where GPER regulated its target genes (c-Fos and connective tissue growth factor gene) and the estrogen-induced migration of CAFs (50). In ovarian cancer, nuclear localization of GPER has been associated with poor survival (54). Nuclear GPER expression has also been associated with poorly differentiated carcinomas and the triple-negative subtype (47). Thus, in the present study, the significance of nuclear GPER in GB required an in-depth experimental approach.

The regulation of GPER expression in GB is currently unknown, to the best of our knowledge. Previous studies have determined that E2 not only increases the expression of GPER mRNA, but also the protein content in different cell
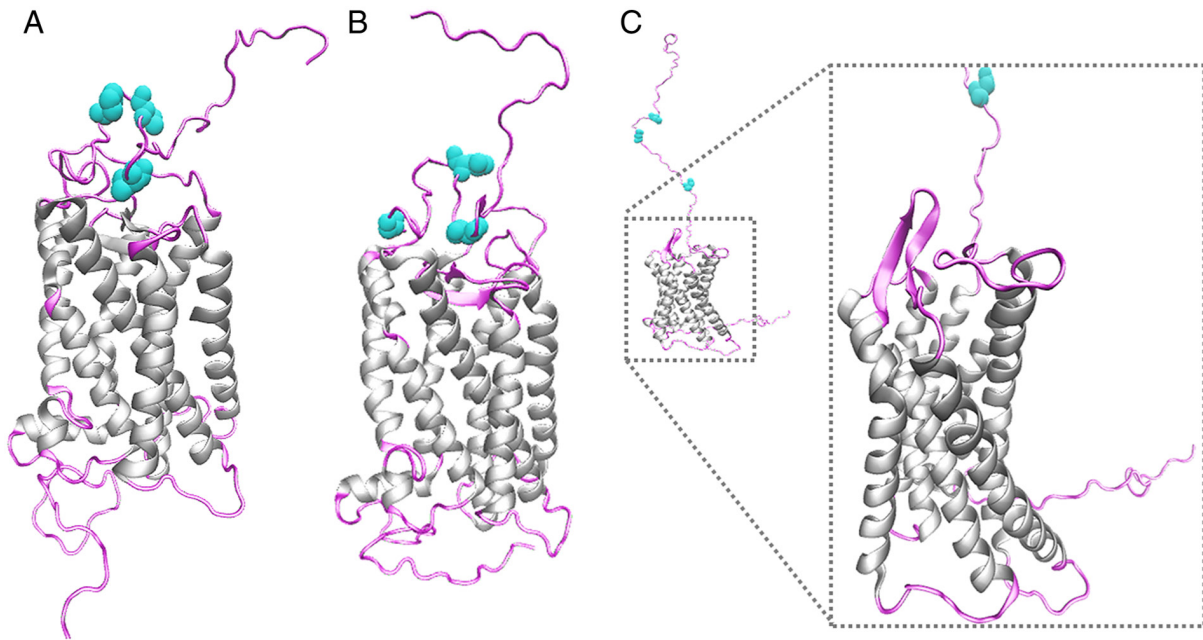
Figure 5. Molecular modeling of GPER. Molecular modeling of GPER using the crystal structures of two bovine rhodopsins: (A) (ID-PDB: 1F88) and (B) (ID-PDB: 1HZX), and a human GPCR (C) (ID: 6LFL) as templates. The structure of GPER is shown, indicating in gray the region of the α-helices corresponding to the seven-transmembrane domains of GPER. The extracellular and intracellular regions are depicted in light pink. Asparagine residues, which are glycosylation targets, were labeled in aqua green. GPER, G-protein coupled estrogen receptor.

types, including endometrial carcinoma cells, chondrocytes, colorectal cells and triple-negative breast cancer cells (55-58). An *in silico* analysis was used to investigate EREs in the GPER gene. This analysis predicted the presence of two EREs in the GPER promoter; however, additional experimental strategies including ChIP or site direct mutagenesis tools are required to confirm the presence of the EREs predicted in this study. Subsequently, to determine the role of E2 in GPER expression, U251, U87, LN229, and T98G cells were treated with various concentrations (1, 10 and 100 nM, and 1 μM). E2 increased GPER content in the U251, U87 and LN229 cells. Of note, in a cell line derived from endometrial adenocarcinoma, E2 increased GPER mRNA levels. Furthermore, the ERα agonist, PPT, induced the same response as E2; this effect was not observed with the ERβ-specific agonist, DPN (55), suggesting that the regulation of GPER expression by E2 is ERα-dependent. The role of E2 in the progression of GBs has been previously reported by the authors. In 2012, González-Arenas *et al* revealed (3) that E2 treatment increased the proliferation of human glioblastoma-derived cell lines. Interestingly, when specific agonists were used for both ER subtypes, only the ERα agonist (PP2) increased proliferation. More recently, Hernández-Vega *et al* (6) reported that E2 promoted epithelial-mesenchymal transition through changes in cell morphology and expression of EMT markers (vimentin and N-cadherin). When the ERα agonist was used, the same effects were observed as those induced by the E2 treatment. However, the ERβ agonist did not promote any events associated with EMT. Notably, in ovarian cancer cells (BG-1), GPER and ERα have been reported to co-operate in order to induce proliferation (15). A possible interaction of these receptors to mediate pro-oncogenic actions of E2 in GB could also occur.

As regards the regulation of GPER expression, Fan *et al* determined that E2 at a concentration of 10 and 100 nM increased the GPER content in chondrocyte-derived cells (56) and different colorectal (HCT116, HT-29 and Caco2) and breast cancer cell lines (triple-negative breast cancer: HCC1806, HCC1937, MDA-MB-231), E2 10 nM increased GPER content (57,58). Subsequently, this condition was evaluated and a wider range of E2 concentrations was analyzed. Aside from this, E2 has diverse effects on the GB depending on its concentration (3,5). It is worth noting that in the experiments performed during the present study, E2 100 nM, did not increase GPER protein content. Our model presents a different cellular context than the one reported by Fan *et al*; it has been previously observed that the activity of GPER, as an atypical GPCR, can vary depending on the species, tissue, and cellular context (59,60). Thus, further studies are required for the definition of the exact E2 range concentrations that may affect GPER content. Moreover, the activation or inhibition of endocytosis after ligand binding and activation to avoid excess cell signaling (52), interaction with other membrane proteins such as clathrin or arrestin (61), or possible receptor dimerization as a desensitization mechanism (62,63), may have an impact on GPER content. Whether E2 may induce some of these cellular processes affecting GPER expression in GB cells, excluding the transcriptional regulation suggested by the presence of the EREs in the GPER promoter, remains to be fully elucidated.

Finally, a GPER-ligand interaction through molecular docking was performed. Three models of the GPER structure were obtained based on two bovine rhodopsin templates (1F88 and 1HZX) and one human GPCR template (6LFL). The analysis predicted that E2 or G1 binding occurs in an extracellular region in 1F88 and 1HZX models and in
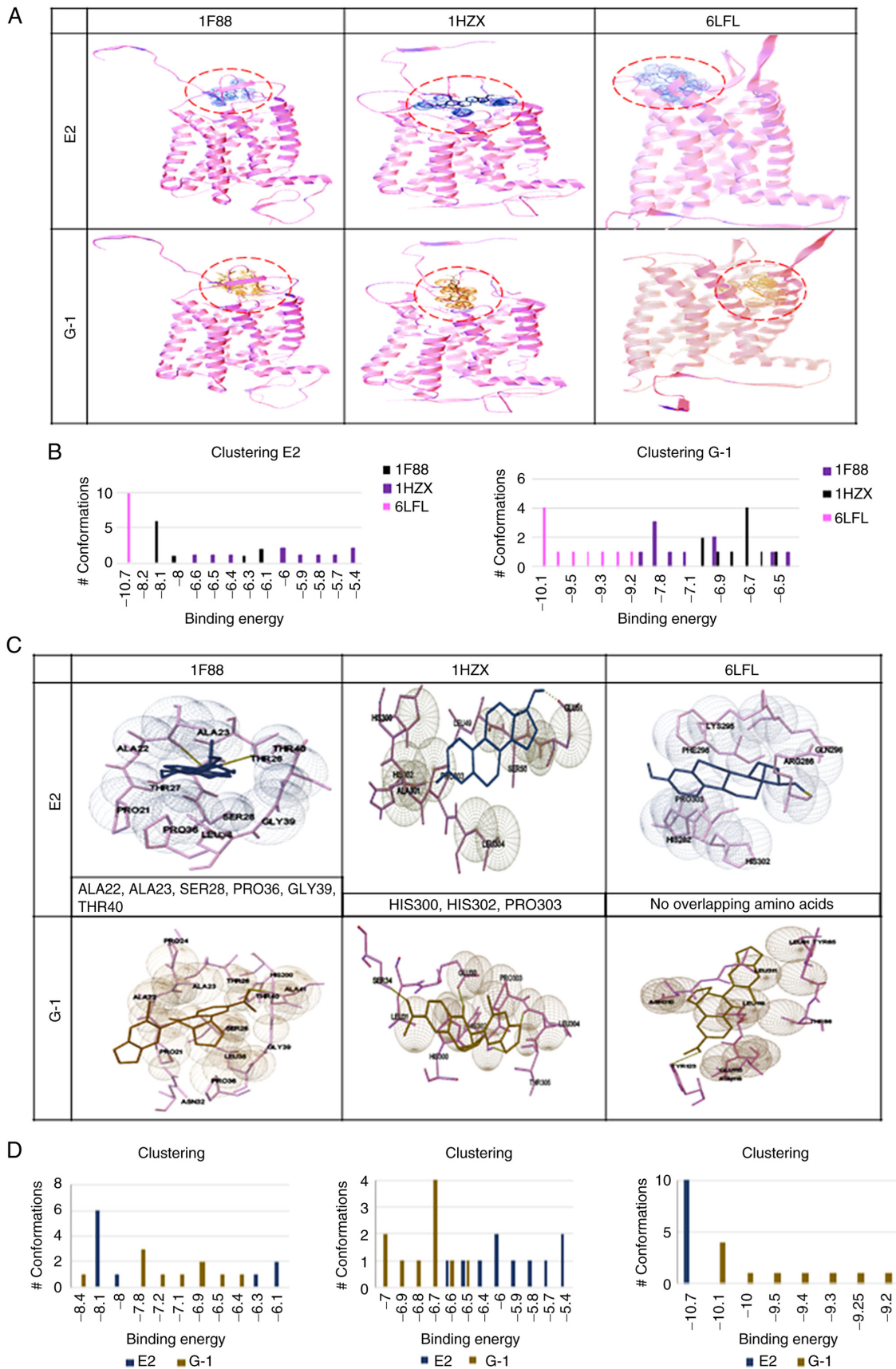
Figure 6. Docking of three GPER models. Docking was obtained with 1F88, 1HZX, and 6LFL in the presence of E2 and G1 ligands. (A) Binding sites for E2 and G1 of each GPER molecular model. A graph is shown for each of the templates used in the analysis. (B) Graphs represent the binding energy values of the corresponding ligand (E2 or G1) according to the three templates used vs. the number of conformations of the corresponding ligand. One graph is included for each group of ligand conformations, E2 or G1. (C) Amino acids involved in the interaction of GPER with E2 or G1 in each one of the templates (1F88, 1HZX, and 6LFL) used. In models 1F88 and 1HZX, the predicted amino acids interacting with E2 and G1 overlap; however, according to 6LFL model, E2 and G1 appear to interact in different regions of GPER. (D) Comparison of the binding energy of the E2 or G1 ligands vs. the number of ligand conformations for each GPER template. GPER, G-protein coupled estrogen receptor; E2, 17 β-estradiol.

a transmembrane region in the 6LFL model. According to the1F88 model, E2 and G1 binding sites share ALA22, ALA23, SER28, PRO36, GLY39 and THR40 residues, suggesting that both ligands may have the same binding site. Similarly, model 1HZX suggested that the binding site for the ligands shares the region comprising HIS300, HIS302, and PRO303 residues. In the human GPCR-based model, there was no overlap in the amino acids involved in E2 or G1 binding, suggesting that E2 and G1 exert different functions when interacting with this receptor. In addition, the highest binding energies for E2 and G1 were detected in the human GPCR-based model (6LFL), suggesting that this is the most realistic model. In this regard, Grande *et al* (64) reported that the interaction of G1 and E2 with GPER occurs in an intracellular region. However, a molecular docking for deciphering the GPER agonist interactions reported that a ligand could be recognized at different binding sites depending on the used structural GPER conformation (65). Variations in structural templates have repercussions on the docking modeling, especially on the first 50 residues of the N-terminal present in the extracellular region and are prone to acquire disordered conformations when modeled by computational methods. Thus, in order to obtain definitive and consistent results of molecular docking of GPER and its ligands, further refinement of the GPER modeling and the resolution of the GPER crystallographic structure is required.

In conclusion, in the present study, the expression of GPER in human astrocytoma (U251) and glioblastoma tumor cell lines (U87, LN229 and T98) at the mRNA and protein level was reported, which was localized in the plasma membrane, cytoplasm, and nucleus. In addition, by performing *in silico* analysis, the presence of two EREs in the promoter region of the GPER gene was described. Interestingly, it was revealed that E2 increased the expression of this receptor at the protein level in human GB-derived cells. Furthermore, by molecular modeling studies, potential three-dimensional structures of GPER were obtained, and by docking analysis, the potential binding sites for their ligands, E2, and its specific agonist G1, were identified. The present study provides the basis for further investigating the role of E2 actions mediated by GPER in GB, which will outline the integrative view of E2 broad actions in GB. Studying the GPER-mediated E2 signaling consequences in GB could contribute to the design of new pharmacological therapies that target specific pro-oncogenic actions modulated by specific E2 subtype receptors.

Availability of data and materials

The datasets used and/or analyzed during the current study are available from the corresponding author on reasonable request.

Authors' contributions

KMPG, KHO, CBA and ICA designed the experiments. KMPG and KHO performed the experiments. KMPG, KHO and CBA confirm the authenticity of all the raw data. KMPG and CBA wrote the first draft preparation; KHO, CBA and ICA contributed to the revision and editing of the manuscript. ICA obtained the funding support. All authors have read and approved the final manuscript.

Ethics approval and consent to participants

Not applicable.

Patient consent for publication

Not applicable.

Competing interests

The authors declare that they have no competing interests.

References

1. Ostrom QT, Cioffi G, Gittleman H, Patil N, Waite K, Kruchko C and Barnholtz-Sloan JS: CBTRUS statistical report: Primary brain and other central nervous system tumors diagnosed in the United States in 2012-2016. Neuro Oncol 21 (Suppl 5): V1-V100, 2019.
2. Bello-Alvarez C and Camacho-Arroyo I: Impact of sex in the prevalence and progression of glioblastomas: The role of gonadal steroid hormones. Biol Sex Differ 12: 28, 2021.
3. González-Arenas A, Hansberg-Pastor V, Hernández-Hernández OT, González-García TK, Henderson-Villalpando J, Lemus-Hernández D, Cruz-Barrios A, Rivas-Suárez M and Camacho-Arroyo I: Estradiol increases cell growth in human astrocytoma cell lines through ERα activation and its interaction with SRC-1 and SRC-3 coactivators. Biochim Biophys Acta 1823: 379-386, 2012.
4. Wan S, Jiang J, Zheng C, Wang N, Zhai X, Fei X, Wu R and Jiang X: Estrogen nuclear receptors affect cell migration by altering sublocalization of AQP2 in glioma cell lines. Cell Death Discov 4: 49, 2018.
5. Altiok N, Ersoz M and Koyuturk M: Estradiol induces JNK-dependent apoptosis in glioblastoma cells. Oncol Lett 2: 1281-1285, 2011.
6. Hernández-Vega AM, Del Moral-Morales A, Zamora-Sánchez CJ, Piña-Medina AG, González-Arenas A and Camacho-Arroyo I: Estradiol induces epithelial to mesenchymal transition of human glioblastoma cells. Cells 9: 1930, 2020.
7. Sareddy GR, Nair BC, Gonugunta VK, Zhang QG, Brenner A, Brann DW, Tekmal RR and Vadlamudi RK: Therapeutic significance of estrogen receptor β agonists in gliomas. Mol Cancer Ther 11: 1174-1182, 2012.
8. Owman C, Blay P, Nilsson C and Lolait SJ: Cloning of human cDNA encoding a novel heptahelix receptor expressed in Burkitt's lymphoma and widely distributed in brain and peripheral tissues. Biochem Biophys Res Commun 228: 285-292, 1996.
9. Revankar CM, Cimino DF, Sklar LA, Arterburn JB and Prossnitz ER: A transmembrane intracellular estrogen receptor mediates rapid cell signaling. Science 307: 1625-1630, 2005.
10. Yue J, Wang XS, Feng B, Hu LN, Yang LK, Lu L, Zhang K, Wang YT and Liu SB: Activation of G - protein-coupled receptor 30 protects neurons against excitotoxicity through inhibiting excessive autophagy induced by glutamate. ACS. Chem Neurosci 10: 4227-4236, 2019.

11. Yu T, Liu M, Luo H, Wu C, Tang X, Tang S, Hu P, Yan Y, Wang Z and Tu G: GPER mediates enhanced cell viability and motility via non-genomic signaling induced by 17β-estradiol in triple-negative breast cancer cells. J Steroid Biochem Mol Biol 143: 392-403, 2014.
12. Liu Y, Ma H and Yao J: ERα, A key target for cancer therapy: A review. Onco Targets Ther 13: 2183-2191, 2020.
13. Chen Y, Tang H, He J, Wu X, Wang L, Liu X and Lin H: Interaction of nuclear ERs and GPER in vitellogenesis in zebrafish. J Steroid Biochem Mol Biol 189: 10-18, 2019.
14. Sánchez DS, Fischer Sigel LK, Azurmendi PJ, Vlachovsky SG, Oddo EM, Armando I, Ibarra FR and Silberstein C: Estradiol stimulates cell proliferation via classic estrogen receptor-alpha and G protein-coupled estrogen receptor-1 in human renal tubular epithelial cell primary cultures. Biochem Biophys Res Commun 512: 170-175, 2019.
15. Vivacqua A, Lappano R, De Marco P, Sisci D, Aquila S, De Amicis F, Fuqua SA, Andò S and Maggiolini M: G protein-coupled receptor 30 expression is upregulated by EGF and TGF alpha in estrogen receptor alpha-positive cancer cells. Mol Endocrinol 23: 1815-1826, 2009.
16. Smith HO, Arias-Pulido H, Kuo DY, Howard T, Qualls CR, Lee SJ, Verschraegen CF, Hathaway HJ, Joste NE and Prossnitz ER: GPR30 predicts poor survival for ovarian cancer. Gynecol Oncol 114: 465-471, 2009.
17. Molina L, Figueroa CD, Bhoola KD and Ehrenfeld P: GPER-1/GPR30 a novel estrogen receptor sited in the cell membrane: Therapeutic coupling to breast cancer. Expert Opin Ther Targets 21: 755-766, 2017.
18. Zhang KS, Chen HQ, Chen YS, Qiu KF, Zheng XB, Li GC, Yang HD and Wen CJ: Bisphenol A stimulates human lung cancer cell migration via upregulation of matrix metalloproteinases by GPER/EGFR/ERK1/2 signal pathway. Biomed Pharmacother 68: 1037-1043, 2014.
19. Avino S, De Marco P, Cirillo F, Santolla MF, De Francesco EM, Perri MG, Rigiracciolo D, Dolce V, Belfiore A, Maggiolini M, et al: Stimulatory actions of IGF-I are mediated by IGF-IR cross-talk with GPER and DDR1 in mesothelioma and lung cancer cells. Oncotarget 7: 52710-52728, 2016.
20. Hirtz A, Lebourdais N, Rech F, Bailly Y, Vaginay A, Smaïl-Tabbone M, Dubois-Pot-Schneider H and Dumond H: GPER Agonist G-1 disrupts tubulin dynamics and potentiates temozolomide to impair glioblastoma cell proliferation. Cells 10: 3438, 2021.
21. Deng J, Wang W, Yu G and Ma X: MicroRNA-195 inhibits epithelial-mesenchymal transition by targeting G protein-coupled estrogen receptor 1 in endometrial carcinoma. Mol Med Rep 20: 4023-4032, 2019.
22. Pfaffl MW: A new mathematical model for relative quantification in real-time RT-PCR. Nucleic Acids Res 29: e45, 2001.
23. Schmittgen TD and Livak KJ: Analyzing real-time PCR data by the comparative C(T) method. Nat Protoc 3: 1101-1108, 2008.
24. Measuring cell fluorescence using ImageJ: https://theolb.readthedocs.io/en/latest/imaging/measuring-cell-fluorescence-using-imagej.html. Accessed September 20, 2021.
25. Khan A, Fornes O, Stigliani A, Gheorghe M, Castro-Mondragon JA, Van Der Lee R, Bessy A, Chèneby J, Kulkarni SR, Tan G, et al: JASPAR 2018: Update of the open-access database of transcription factor binding profiles and its web framework. Nucleic Acids Res 46(D1): D260-D266, 2018.
26. Heinz S, Benner C, Spann N, Bertolino E, Lin YC, Laslo P, Cheng JX, Murre C, Singh H and Glass CK: Simple combinations of lineage-determining transcription factors prime cis-regulatory elements required for macrophage and B cell identities. Mol Cell 38: 576-589, 2010.
27. Kulakovskiy IV, Vorontsov IE, Yevshin IS, Sharipov RN, Fedorova AD, Rumynskiy EI, Medvedeva YA, Magana-Mora A, Bajic VB, Papatsenko DA, et al: HOCOMOCO: Towards a complete collection of transcription factor binding models for human and mouse via large-scale ChIP-Seq analysis. Nucleic Acids Res 46(D1): D252-D259, 2018.
28. Tan G and Lenhard B: TFBSTools: An R/bioconductor package for transcription factor binding site analysis. Bioinformatics 32: 1555-1556, 2016.
29. Thorvaldsdóttir H, Robinson JT and Mesirov JP: Integrative genomics viewer (IGV): High-performance genomics data visualization and exploration. Brief Bioinform 14: 178-192, 2013.
30. Pettersen EF, Goddard TD, Huang CC, Couch GS, Greenblatt DM, Meng EC and Ferrin TE: UCSF Chimera-A visualization system for exploratory research and analysis. J Comput Chem 25: 1605-1612, 2004.
31. Webb B and Sali A: Comparative protein structure modeling using MODELLER. Curr Protoc Bioinformatics 54: 5.6.1-5.6.37, 2017.
32. Sánchez R and Šali A: Comparative Protein Structure Modeling in Genomics. In: Methods in Molecular Biology. Sánchez R and Sali A (eds.). Vol. 143. Humana Press Inc., Totowa, NJ, pp97-127, 1999.
33. Finn RD, Clements J and Eddy SR: HMMER web server: Interactive sequence similarity searching. Nucleic Acids Res 39(Web Server Issue): W29-W37, 2011.
34. Wiederstein M and Sippl MJ: ProSA-web: Interactive web service for the recognition of errors in three-dimensional structures of proteins. Nucleic Acids Res 35(Web Server Issue): W407-W410, 2007.
35. Humphrey W, Dalke A and Schulten K: VMD: Visual molecular dynamics. J Mol Graph 14: 33-8, 27-8, 1996.
36. Goodsell DS, Sanner MF, Olson AJ and Forli S: The AutoDock suite at 30. Protein Sci 30: 31-43, 2021.
37. O'Boyle NM, Banck M, James CA, Morley C, Vandermeersch T and Hutchison GR: Open Babel: An open chemical toolbox. J Cheminform 3: 33, 2011.
38. Bitencourt-Ferreira G, Pintro VO and de Azevedo WF Jr: Docking with AutoDock4. Methods Mol Biol 2053: 125-148, 2019.
39. Azizian H, Khaksari M, Asadi karam G, Esmailidehaj M and Farhadi Z: Cardioprotective and anti-inflammatory effects of G-protein coupled receptor 30 (GPR30) on postmenopausal type 2 diabetic rats. Biomed Pharmacother 108: 153-164, 2018.
40. Pupo M, Bodmer A, Berto M, Maggiolini M, Dietrich PY and Picard D: A genetic polymorphism repurposes the G-protein coupled and membrane-associated estrogen receptor GPER to a transcription factor-like molecule promoting paracrine signaling between stroma and breast carcinoma cells. Oncotarget 8: 46728-46744, 2017.
41. Gonzalez de Valdivia E, Sandén C, Kahn R, Olde B and Leeb-Lundberg LMF: Human G protein-coupled receptor 30 is N-glycosylated and N-terminal domain asparagine 44 is required for receptor structure and activity. Biosci Rep 39: BSR20182436, 2019.
42. Buruiană A, Florian ȘI, Florian AI, Timiș TL, Mihu CM, Miclăuș M, Oșan S, Hrapșa I, Cataniciu RC, Farcaș M and Șușman S: The roles of miRNA in glioblastoma tumor cell communication: Diplomatic and aggressive negotiations. Int J Mol Sci 21: 1950, 2020.
43. Robertson FL, Marqués-Torrejón MA, Morrison GM and Pollard SM: Experimental models and tools to tackle glioblastoma. Dis Model Mech 12: dmm040386, 2019.
44. Brennan CW, Verhaak RG, McKenna A, Campos B, Noushmehr H, Salama SR, Zheng S, Chakravarty D, Sanborn JZ, Berman SH, et al: The somatic genomic landscape of glioblastoma. Cell 155: 462-477, 2013.
45. Yan Y, Liu H, Wen H, Jiang X, Cao X, Zhang G and Liu G: The novel estrogen receptor GPER regulates the migration and invasion of ovarian cancer cells. Mol Cell Biochem 378: 1-7, 2013.
46. Gonzalez de Valdivia E, Broselid S, Kahn R and Leeb-lundberg LMF: G protein-coupled estrogen receptor 1 (GPER1)/GPR30 increases ERK1/2 activity through PDZ motif-dependent and -independent mechanisms. J Biol Chem 292: 9932-9943, 2017.
47. Samartzis EP, Noske A, Meisel A, Varga Z, Fink D and Imesch P: The G protein-coupled estrogen receptor (GPER) is expressed in two different subcellular localizations reflecting distinct tumor properties in breast cancer. PLoS One 9: e83296, 2014.
48. Sjöström M, Hartman L, Grabau D, Fornander T, Malmström P, Nordenskjöld B, Sgroi DC, Skoog L, Stål O, Leeb-Lundberg LM and Fernö M: Lack of G protein-coupled estrogen receptor (GPER) in the plasma membrane is associated with excellent long-term prognosis in breast cancer. Breast Cancer Res Treat 145: 61-71, 2014.
49. Madeo A and Maggiolini M: Nuclear alternate estrogen receptor Gpr30 mediates 17beta-estradiol-induced gene expression and migration in breast cancer-associated fibroblasts. Cancer Res 70: 6036-6046, 2010.
50. Pupo M, Vivacqua A, Perrotta I, Pisano A, Aquila S, Abonante S, Gasperi-Campani A, Pezzi V and Maggiolini M: The nuclear localization signal is required for nuclear GPER translocation and function in breast cancer-associated fibroblasts (CAFs). Mol Cell Endocrinol 376: 23-32, 2013.
51. Cheng SB, Quinn JA, Graeber CT and Filardo EJ: Down-modulation of the G-protein-coupled estrogen receptor, GPER, from the cell surface occurs via a trans-Golgi-proteasome pathway. J Biol Chem 286: 22441-22455, 2011.

52. Figueira MI, Cardoso HJ and Socorro S: The role of GPER signaling in carcinogenesis: A focus on prostate cancer. In: Recent Trends in Cancer Biology: Spotlight on Signaling Cascades and microRNAs. Fayyaz S and Farooqi A (eds.). Springer, Cham, pp59-117, 2018.

53. Innamorati G, Le Gouill C, Balamotis M and Birnbaumer M: The long and the short cycle. Alternative intracellular routes for trafficking of G-protein-coupled receptors. J Biol Chem 276: 13096-13103, 2001.

54. Zhu CX, Xiong W, Wang ML, Yang J, Shi HJ, Chen HQ and Niu G: Nuclear G protein-coupled oestrogen receptor (GPR30) predicts poor survival in patients with ovarian cancer. J Int Med Res 46: 723-731, 2018.

55. Plante BJ, Lessey BA, Taylor RN, Wang W, Bagchi MK, Yuan L, Scotchie J, Fritz MA and Young SL: G protein-coupled estrogen receptor (GPER) expression in normal and abnormal endometrium. Reprod Sci 19: 684-693, 2012.

56. Fan DX, Yang XH, Li YN and Guo L: 17β-estradiol on the expression of G-Protein coupled estrogen receptor (GPER/GPR30) mitophagy, and the PI3K/Akt signaling pathway in ATDC5 chondrocytes in vitro. Med Sci Monit 24: 1936-1947, 2018.

57. Gilligan LC, Rahman HP, Hewitt AM, Sitch AJ, Gondal A, Arvaniti A, Taylor AE, Read ML, Morton DG and Foster PA: Estrogen activation by steroid sulfatase increases colorectal cancer proliferation via GPER. J Clin Endocrinol Metab 102: 4435-4447, 2017.

58. Huang R, Li J, Pan F, Zhang B and Yao Y: The activation of GPER inhibits cells proliferation, invasion and EMT of triple-negative breast cancer via CD151/miR-199a-3p bio-axis. Am J Transl Res 12: 32-44, 2020.

59. Prossnitz ER and Arterburn JB: International union of basic and clinical pharmacology. XCVII. G protein-coupled estrogen receptor and its pharmacologic modulators. Pharmacol Rev 67: 505-540, 2015.

60. Luo J and Liu D: Does GPER really function as a G protein-coupled estrogen receptor in vivo?. Front Endocrinol (Lausanne) 11: 148, 2020.

61. Jala VR, Radde BN, Haribabu B and Klinge C: Enhanced expression of G-protein coupled estrogen receptor (GPER/GPR30) in lung cancer. BMC Cancer 12: 624, 2012.

62. Milligan G, Canals M, Pediani JD, Ellis J and Lopez-Gimenez JF: The role of GPCR Dimerisation/Oligomerisation in receptor signalling. Ernst Schering Found Symp Proc 2: 145-161, 2006.

63. Gurevich VV, and Gurevich EV: How and why do GPCRs dimerize?. Trends Pharmacol Sci 29: 234-240, 2008.

64. Grande F, Occhiuzzi MA, Lappano R, Cirillo F, Guzzi R, Garofalo A, Jacquot Y, Maggiolini M, Rizzuti B: Computational approaches for the discovery of GPER targeting compounds. Front Endocrinol (Lausanne) 11: 517, 2020.

65. Méndez-Luna D, Martínez-Archundia M, Maroun RC, Ceballos-Reyes G, Fragoso-Vázquez MJ, González-Juárez DE and Correa-Basurto J: Deciphering the GPER/GPR30-agonist and antagonists interactions using molecular modeling studies, molecular dynamics, and docking simulations. J Biomol Struct Dyn 33: 2161-2172, 2015.